Article:

Ma, WL, Wang, HX, Barker, R et al. (3 more authors) (2021) Corrosion behaviour of X65 carbon steel under the intermittent oil/water wetting: A synergic effect of flow velocity and alternate immersion period. Corrosion Science, 187. 109507. ISSN 0010-938X

https://doi.org/10.1016/j.corsci.2021.109507

Corrosion behaviour of X65 carbon steel under the intermittent oil/water wetting: A synergic effect of flow velocity and alternate immersion period

Wen Long Ma[a,b], Han Xiang Wang[a], Richard Barker[b], Nikil Kapur[b], Yong Hua[b]* and Anne Neville[b]*

[a] School of Mechanical Engineering, China University of Petroleum (East China), Qingdao, 266555, China

[b] School of Mechanical Engineering, University of Leeds, Leeds, LS2 9JT, United Kingdom

**Corresponding authors:*
Yong Hua: Y.Hua@leeds.ac.uk;
Han Xiang Wang: Wanghx1899@163.com

Abstract:

The effect of flow on corrosion behaviour of carbon steel under intermittent oil/water wetting was investigated by a newly-modified "alternate wetting cell", combining with the use of potentiostatic polarisation, *in-situ* visualisation, contact angle measurements and scanning electron microscopy (SEM). The oil/water wetting time was determined by the formation of a thin oil/water film on the electrode surface after the transition of immersion state. A short alternate oil/water immersion period and low flow velocity can increase the ratio (oil to water wetting time) and efficiently mitigate the corrosion, proposing a logistic regression tendency between corrosion mitigation efficiency and oil/water wetting time.

Keywords: *Carbon steel, CO_2 corrosion, Current-time curve, Wetting hysteresis*

1. Introduction

In the oil and gas industry, the cost of corrosion of downhole strings and transportation pipelines is significant and involves the replacement of construction materials, downtime, and potential environmental pollution [1, 2]. To better understand and control corrosion of the materials exposed to multiphase oil/water corrosive media, significant research [3-15] has been conducted, it has reported that the presence of oil can reduce the corrosion rate of steel via forming a protective oil film on the surface, acting as a barrier to restrict the corrosive species pathway. Other mechanisms for mitigating against corrosion include soluble chemical portioning [13-14] and water entrainment [4-12, 15].

The cut (or fraction) of water within the flow strongly influences the degree of corrosion. At water cuts below 50%, the formation of the water-in-oil emulsion is typical, which substantially mitigates corrosion due to the low conductivity of the continuous oil phase [16]. The corrosion morphology of steel under such circumstances can exist in the form of localised corrosion [4, 8-9, 14-15], which implies that a small amount of water can wet the steel surface and initiate the corrosion locally. When the water cut increases up to 90% and water becomes the continuous phase, the corrosion rate greatly increases and mesa-type localized corrosion occurs on the steel surface [4, 10-11, 14-15]. The observed grinding marks after corrosion tests illustrate that the oil droplets/films locally covered the steel surface and greatly prevent corrosion [10-11]. The wetting of the steel surface in the multiphase oil/water flow is complicated and significantly influences corrosion behaviour.

Previous research [4, 10] has identified the critical water cut of 50% based on the measurement of corrosion rate in the oil/water emulsion, but there is a need to further understand the complex effect of wetting behaviour on corrosion. The type of oil/water emulsion is determined by the liquid-liquid (oil-water) interaction, however, wetting behaviour depends on liquid-liquid-solid (oil-water-steel) interaction [3]. It is suggested that the corrosion behaviour of carbon steel exposed to the multiphase oil/water flow is determined by various wetting factors. The wetting state within a transportation pipeline mainly consists of three types: oil-wetting, water-wetting and intermittent oil/water wetting [17-20]. Intermittent wetting is a common wetting state which occurs within the pipelines and this depends on the exact flow pattern within the pipe. For example, the pipeline surface near the oil/water interface with the wavy stratified oil/water flow is alternate oil/water wetting [21]. However, for the oil/water slug flow, the top side of the pipeline is intermittently wetted [22]. With a water-in-oil emulsion, the bottom of the pipeline is alternately wetted by the water droplet or globule [17-20].

Key studies [19, 21, 23-25] have given a good insight into the corrosion of carbon steel under intermittent wetting. Nesic et al. [23] devised a horizontal rotating cylinder (HRC) for studying the effect of water wetting on corrosion of carbon steel in a multiphase oil/water system. Their immersed cylinder sample was half in the hexane and the other half was in the water. Therefore, when the cylinder began to rotate, the steel surface was cyclically wetted by water and oil. The HRC was used by Tang [19] to investigate the combined effect of dynamic wetting and surface roughness on the corrosion of mild steel. The experimental results show that the contact angle under the static condition can not reflect the real wetting state of the surface. Schmitt et al. [21] simulated intermittent oil/water wetting by moving test sample up and down in a stagnant and stratified oil/water solution, in order to investigate the effect of corrosion inhibitor on pitting near the wavy oil/water boundary region of the pipeline. They found that the increase in the frequency of the wetting cycles accelerated localised corrosion in the oil/water interface. Additionally, Babic [24] tested the rotating cylinder electrode (RCE) in a stratified oil/water solution, which achieved the intermittent wetting of the RCE sample. They investigated the effect of pre-corroded surface, implying that the application of RCE is beneficial to record and observe fluidic behaviour. In addition to the above research, Wang et al [25] systematically investigated the corrosion behaviour of carbon steel under alternate oil/water wetting processes. The new "alternate slug model" based on the analysis of experimental observation [26] of pressure variation in an oil/water flow was put forward. Based on the model, an "alternate wetting cell" was developed, which consisted of a rotating disk electrode (RDE), piston, two connected containers and motor. When the piston moved up and down in one container, the height of the oil/water interface was adjusted in the other container. Consequently, a controllable intermittent wetting of the electrode can be achieved. Then the potentiostatic polarization method was applied, and the results show that the low flow velocity or the increase in the frequency of alternate wetting contributed to corrosion mitigation. However, the flow distribution on the surface of the RDE sample increases with the radius, resulting in the influence of the wetting distribution as well as localised corrosion on the surface of the sample during intermittent oil/water wetting which needs further investigation.

During the process of dynamic wetting, wetting hysteresis is a common fluidic behaviour, which is caused by the small defects of solid surface, that is, the contact angle obtained by the advancing meniscus over the substrate is larger than the contact angle for a meniscus that has been receding [28]. Refer to the literature, the effect of wetting hysteresis on the corrosion behaviour during intermittent oil/water wetting phenomenon has not been studied in previous research.

Therefore, a simple and newly modified apparatus to simulate intermittent oil/water wetting, based on Wang's [25] design of the "alternate wetting cell" was developed. Compared with the previous rigs [23, 25], the use of RCE in this current work not only contributing to characterise the peripheral velocity during the intermittent oil/water wetting but also accurately recorded fluidic behaviour at the electrode surface. Furthermore, the potentistatic polarization method was applied to measure the corrosion behaviour of carbon steel under intermittent oil/water wetting. During the intermittent wetting process, a camera and KSV-200 contact angle meter was used to record fluidic behaviour at the material surface. The current study revealed a synergic effect of flow velocity and alternate immersion period on the corrosion behaviour, indicating a relationship between wetting hysteresis and the lifetime of water/oil film at various flow velocities on the corrosion behaviour, with a combination of statistical analysis of current-time curve, recordings of fluidic behaviour and SEM images of the corrosion morphology.

2. Experimental procedure

2.1. Experimental design concept

The intermittent wetting occurs within the pipeline under various flow patterns, the simplified oil or water slug intermittently contacts with the pipeline surface is provided in Figure 1. As shown in Figure 1(a), the wetting state of the test point (red) can be theoretically changed with the alternate switch between oil immersion and water immersion [29-30]. During this switching process between oil slug (L_o) and water slug (L_w), there exists wetting hysteresis at the test point, due to the dynamic contact angle at the interface between the fluid and the wall with a large contact line velocity v. Therefore, the actual wetting time of the test point can be varied, which is shown in Figure 1(b). In order to better understand the difference, t_o and t_w are separately defined as immersion period of oil slug and water slug, whereas t_{ao} and t_{aw} represent the actual wetting times in oil and water, respectively. This immersion period is a controllable independent variable, but the actual wetting time is a measured dependent variable, which can be described through the implementation of potentiostatic polarisation which is an electrochemical method.

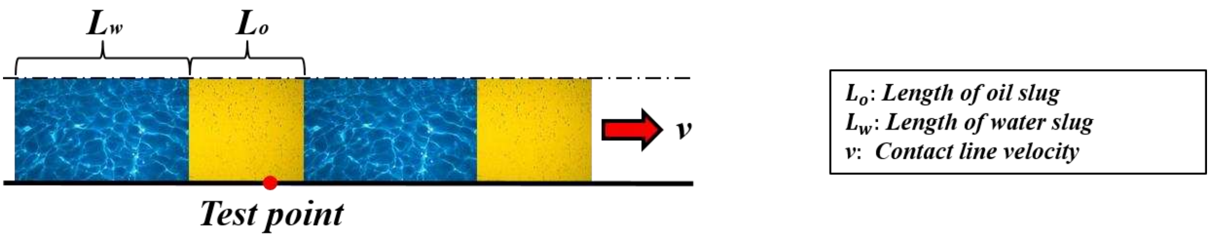

(a)

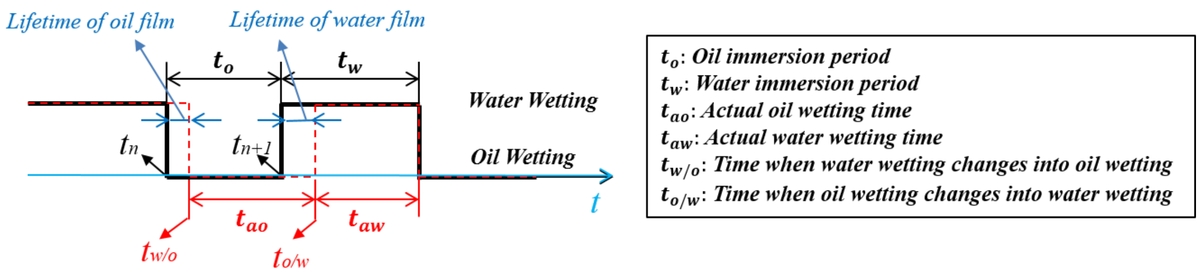

(b)

Figure 1. An illustration of "alternate oil/water slug model" [25]: (a) a schematic of a simplified oil/water slug model, (b) the actual wetting behaviour on the surface. The black solid line represents the contact line position assuming no hysteresis, and the red dash line represents the actual contact line.

2.2. Material and solution preparation

The chemical composition of the carbon steel specimen is shown in Table 1. X65 carbon steel specimens were machined into the cylinder with an outer diameter of 12 mm and a height of 10 mm, which could be mounted to the shaft of the RCE (Figure 2). The RCE electrode was wet-ground up to 600 grit finish using silicon carbide paper, followed by rinsing with acetone and distilled water and drying gently with compressed air.

Table 1: Elemental composition of X65 steel (wt.%).

C	P	Si	Cr	Mn	Ni	S	Mo
0.12	0.008	0.18	0.11	1.27	0.07	0.002	0.17
Cu	B	Sn	Ti	Al	Nb	V	Fe
0.12	0.0005	0.008	0.001	0.022	0.054	0.057	Balance

A mineral oil ($viscosity = 14.71\ \mathrm{mPa \cdot s}$ at 25 °C) instead of crude oil was used within the current study due to the composition of crude oil which can complicate the corrosion processes at the steel surface. Besides, CO_2-saturated 1 wt. % NaCl was used which agrees with the previous intermittent wetting study conducted by the Institute for Corrosion and Multiphase Technology (ICMT) in Ohio University [17-20]. In order to deoxygenate the oil and solution, both mediums were bubbled with CO_2 gas for more than 12h in advance, as well as during the entire experiment.

Based on the "alternate oil/water slug" model, an experimental rig that simulates the intermittent oil/water wetting was designed and can be referred to as an "alternate wetting cell". As shown in Figure 2, the whole system mainly consisted of a rotating cylinder electrode (RCE), a digital gear pump, two hotplates and two glass beakers (Beaker1 was 500 mL, Beaker2 was 1000 mL). Beaker1 is used for the *in-situ* electrochemical measurements during the intermittent oil/water wetting, and Beaker2 contains CO_2-saturated solutions. The brine in two beakers was connected by a gear pump and associated tubes. The experimental procedure was designed carefully, firstly, 250 mL CO_2-saturated solution was added into Beaker1, then 100 mL oil was gently injected, which allowed the electrode to be fully immersed in the oil phase. Under the control of Labview, the use of a gear pump transferred the water phase from one beaker to the other, which enabled the RCE electrode to be intermittently immersed in oil or water. More technical details involving apparatus and Labview parameters are provided in Part 1-2 of the *Appendix*.

In the present study, the oil immersion period was the same as the water immersion period, and 5, 10 and 60 s were selected, according to the measurement of oil/water flow in the pipe [22, 31].

For the dynamic conditions, the rotating speeds of the RCE, 0, 500, 1000 and 1500 rpm were considered, which represents flow velocity of 0, 0.275, 0.597 and 0.971 m/s in a 0.1 m-inside-diameter pipe [17-20, 32] (For details, please see in Part 3 of the *Appendix*). At the static condition, it is convenient to record fluidic behaviour on the surface of the electrode, which contributes to understanding corrosion characterisation of carbon steel under intermittent wetting. The results under the static condition are compared with that of dynamic conditions. All the experiments were conducted at 25°C and each test was repeated at least 3 times.

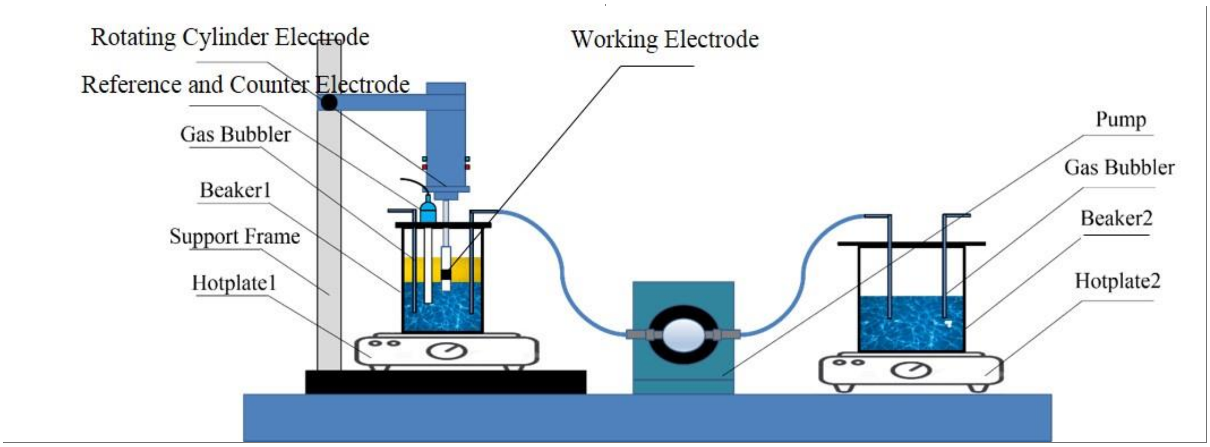

Figure 2. Schematic of “Alternate wetting cell”.

2.3 Electrochemistry measurements

As shown in Figure 2, a standard three-electrode cell was used in this study, which consisted of an RCE electrode made of carbon steel (working electrode, WE), a saturated Ag/AgCl electrode (reference electrode, RE) and a platinum electrode (counter electrode, CE). The RE and CE were immersed in the CO_2-saturated solution during the intermittent wetting processes.

As for the electrochemical methods, open circuit potential (OCP) of the RCE electrode in the CO_2-saturated brine was firstly measured for at least 10 mins until it became stable. Then the potentiostatic polarization method was used to measure the current of WE for 240 min under intermittent oil/water wetting. The applied potential was at + 10 mV vs. OCP, which allows a current to be monitored without greatly damaging the steel surface. In order to precisely measure the time of oil or water wetting, sampling time was set at 0.1s. The electrochemical measurement was conducted using an Ivium-n-stat.

2.3.1 Link the current-time curve to the wetting behaviour

To process the current-time curves obtained by the potentostatic method, the numerical fitting with the equivalent circuit was analysed from EIS data (AC excitation amplitude of 10 mV and frequency range from 10 KHz to 0.1 Hz) where the RCE electrode is immersed in water or oil (Figure 3a). The equivalent circuit that fitted the impedance curve consists of solution resistance (R_s), charge transfer resistance (R_{ct}) and double layer capacity (C_{dl}). The equivalent circuit can be regarded as a circuit with a switch under a constant potential (+10 mV vs. OCP).

According to the proposed circuit, the fundamental unit of current-time curves can be easily understood. As shown in Figure 3(b), when the sample is wetted by an oil slug, the current is 0 mA. However, when the sample changed from oil wetting to water wetting, the current surges to a peak then drops to a steady-state. Such current behaviour is a result of the charging process of the double layer of the sample in the CO_2-saturated solution. A positive current not only represents water wetting but also reflects the corrosion process of the electrode. However, it should be noted that the peak current is a non-Faradic current, which does not involve any chemical reaction [25].

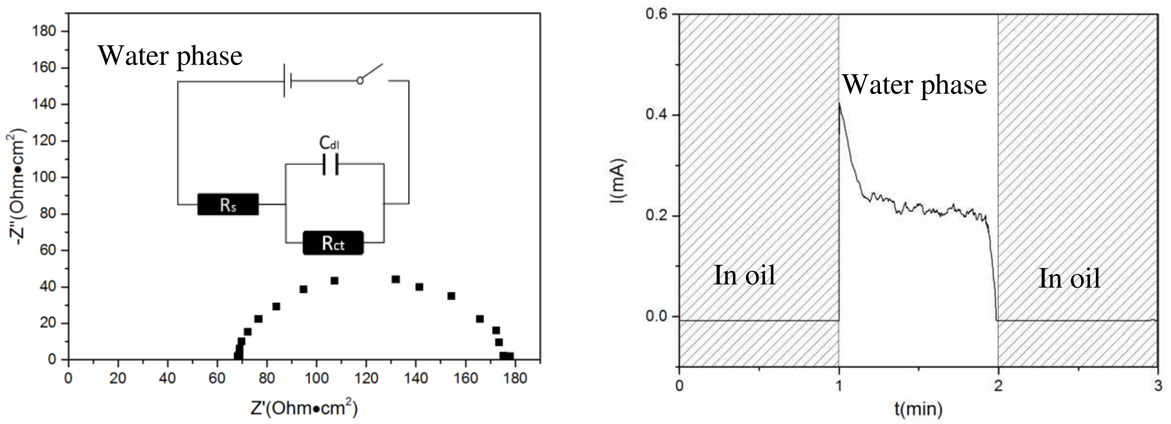

(a) (b)

Figure 3. Analysis of fundamental unit of the current-time curve. (a) EIS of RCE electrode immersed in the water slug and circuit model represents the whole system during the oil-water transition, (b) a current-time curve during the oil-water transition. Shadow area represents oil immersion state, the blank area represents water immersion state.

2.4 Surface analysis

SEM images of the sample surface after the experiment were acquired using a Carl Zeiss EVO MA15 scanning electron microscope (SEM), where a 20 keV accelerating voltage were used. A camera was used to record the fluidic behaviour of the RCE electrode. A KSV CAM 200 contact angle meter was also applied to record the wetting behaviour of the RCE electrode under static conditions, which was alternately immersed in an oil/water slug in a transparent plexiglass box.

2.5 Statistical analysis of the current-time curve

In order to quantitatively study the corrosion behaviour of carbon steel under intermittent wetting phenomenon, three metrics were applied. The proposed dissolution mitigation efficiency (DME, η) was used in the present paper. As shown by Eq. (1), DME was introduced to reflect the mitigation of anodic current in the intermittent oil/water wetting phenomenon compared to its corresponding one in the aqueous solution [33].

$$\eta = \left(1 - \frac{\int_{t_0}^{t_1} I(t)}{\frac{t_1 - t_0}{t_0}\int_0^{t_0} I_0(t)}\right) \times 100\% \quad (1)$$

where t_0 is the time when the intermittent wetting began, t_1 is the time at the end of the whole electrochemical test, $I_0(t)$ is the measured anodic current of an electrode immersed in the solution at initial 60s, and $I(t)$ represent the anodic current measured under intermittent wetting. The measured peak current was replaced by the average current for the same immersion period because that reflects non-Faradic current instead of anodic dissolution of the electrode.

The extent of corrosion mitigation is dependent on the wetting state of the electrode during the intermittent wetting process. Therefore, the ratio between oil wetting time and water wetting time (θ) was calculated below:

$$\theta = \frac{t_{oil}}{t_{water}} \quad (2)$$

where t_{oil} is the sum of time when the current is 0 mA during the whole process of intermittent wetting, and t_{water} represents the sum of time when the current is above 0 mA. If there is no wetting hysteresis, the ratio is 1. According to the recording of fluidic behaviour of the RCE electrode (Figure 5 and Video1-7 of the *Appendix*), wetting hysteresis under intermittent oil/water wetting is caused by the existence of the oil or water film after the transition between different immersion states. The lifetime of the liquid film plays an important role in the wetting state of the electrode, which consequently influences corrosion behaviour. Therefore, the lifetime of the liquid film will be analysed through Eq. (3) and (4):

$$Lifetime\ of\ oil\ film = \begin{cases} t_{o/w} - t_n & when\ current\ becomes\ positive\ during\ n^{th}\ water\ immersion\ period \\ t_w & when\ current\ keeps\ 0\ \ during\ n^{th}\ water\ immersion\ period \end{cases} \quad (3)$$

$$Lifetime\ of\ water\ film = \begin{cases} t_{w/o} - t_n & when\ current\ becomes\ 0\ during\ n^{th}\ oil\ immersion\ period \\ t_o & when\ current\ keeps\ positive\ \ during\ n^{th}\ oil\ immersion\ period \end{cases} \quad (4)$$

where $t_{o/w}$ represents the time when the current becomes positive from 0 mA, $t_{w/o}$ represents the time when current drops to 0 mA from the positive one (Figure 1(b)), t_n is the start time of the n^{th} oil or water immersion period, t_o and t_w separately represents oil immersion and water immersion period. The above data analysis method was conducted by combination analysis of Excel and MATLAB.

3. Results

3.1. Validation of the testing rig

The electrochemical potentiostatic polarisation data of the RCE test in the CO_2-saturated solution under different rotating speeds were measured. Figure 4(a) indicates that the current of the sample immersed in the CO_2-saturated solution was about $220\ \mu A$ for 240 mins under the static condition. As shown in Figure 4(b), the steady current-time curves were also observed at various rotating speeds, the currents have no significant influence at various rotating speeds, which is in good agreement with previous research [25, 34]. The steady-state OCP of the electrode under the static condition was -0.675 V (vs Ag/AgCl) at 25°C. As the increase in the rotating speed, the OCP values rise to the ranges between -0.655 V and -0.660 V.

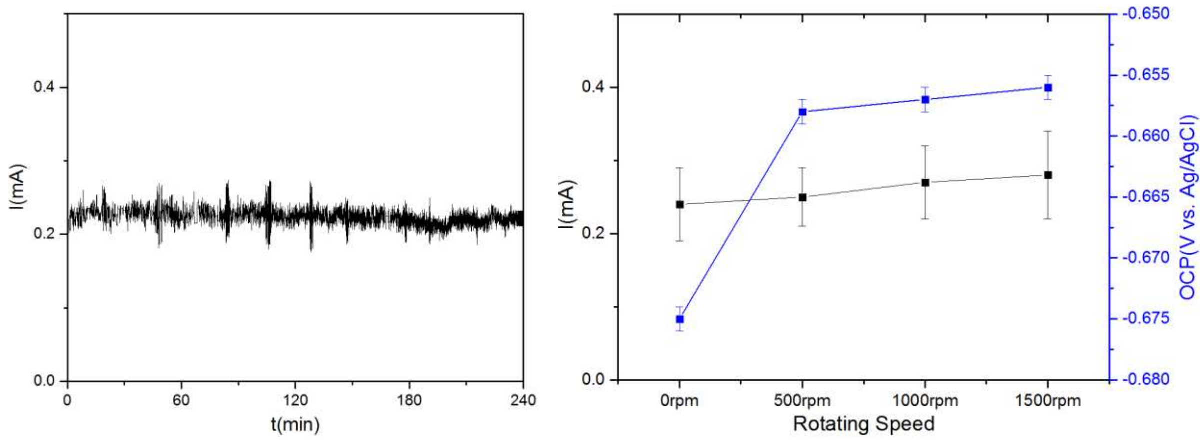

(a) (b)

Figure 4. Current-time curves of the RCE electrode immersed in the CO_2-saturated solution. (a) the current-time curve at 0 rpm, (b) average current and OCP of RCE electrode at different rotating speeds.

Figure 5 indicates the typical current-time segments of carbon steel exposed to alternate oil/water wetting. As shown in Figure 5(a), the characteristic of the current-time curve was an instant on-off mode, more specifically, when the sample changed from water immersion to oil immersion, the currents sharply dropped to 0 mA. Under the contrary transition from oil immersion to water immersion, resulting in the current instantly risng. The above current-time curve indicates that the wetting state of the sample changes with the transition of immersion state. Based on visual observations obtained by the camera, the water wetting sample was covered by oil droplets of various sizes (Photo 1 of Figure 5(a)), leading to a small reduction of anodic current. More details can be observed in Video 1 in Part4 of the *Appendix*.

As shown in Figure 5(b), the sample changed from oil immersion to water immersion at the 4th minute, the current remained 0 mA for 10 s, suddenly increased to the peak and then dropped to the steady-state. It is interesting to note that the current was measured at 0 mA for the whole alternate immersion period (60s) at the 6th minute. The recording of fluidic behaviour at the sample surface after the transition helps to interpret current behaviour. As shown in Photo 2 of Figure 5(b) and Video 2 in Part 4 of the *Appendix*, though the sample was immersed in the CO_2-saturated solution after the transition, the sample was still fully covered by a thin oil film, which prevented the corrosion of the surface. Therefore, the oil wetting time was thereby extended. However, due to the surface tension and molecular forces in the oil/water/steel three-phase system [35], the oil film ruptured, and the sample instantly contacted with the CO_2-saturated solution, which switched on the circuit, causing the current to immediately become positive.

The measured current was extended after the transition from water immersion to oil immersion as shown in Figure 5(c), the current dropped to 0.02 mA instead of 0 mA after the 70s. Observation of the fluid during the transition process (Photo 2 of Figure 5(c) and Video 4 in Part4 of the *Appendix*) shows the remaining water film formed on the sample surface still allowed current flow. The results reveal a strong correlation between the measured current and wetting state of electrode surface using the present rig, which helps to understand the corrosion behaviour of the sample.

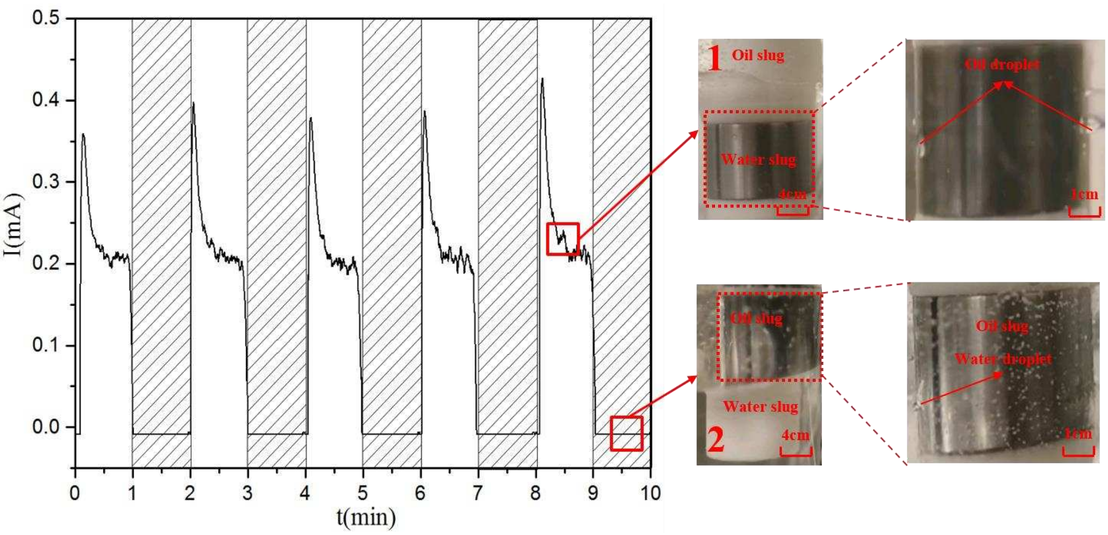

(a)

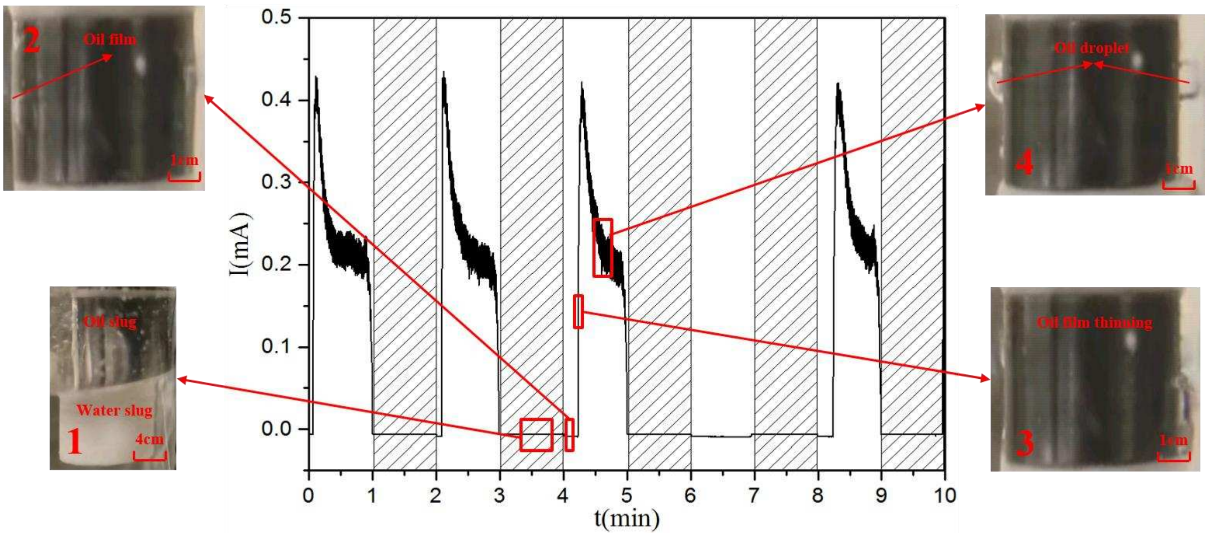

(b)

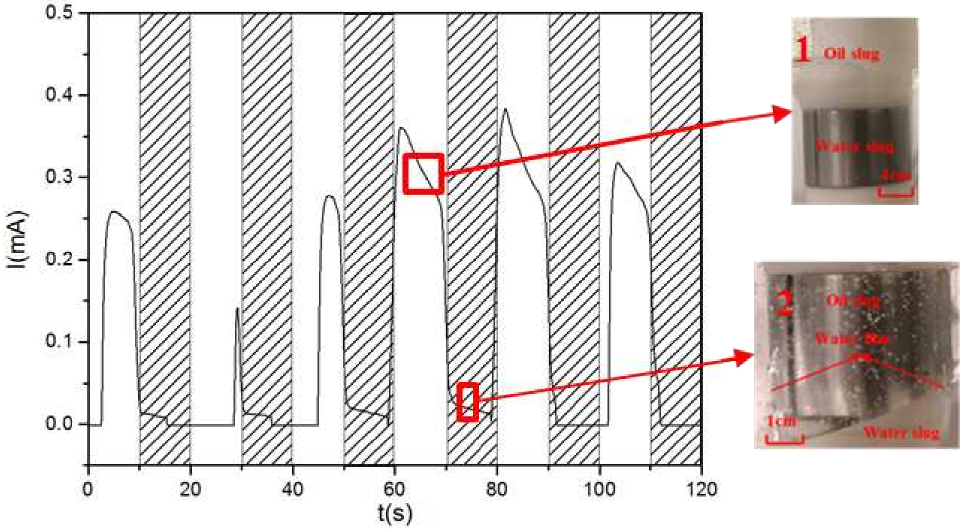

(c)

Figure 5. Typical transient current-time segment and recording of fluidic behaviour of RCE electrode at 0 rpm in oil/water alternate wetting of different alternate immersion period. (a) Instant on-off mode at 60s, (b) On-off mode with hysteresis caused by an oil film at 60s, (c) on-off mode with hysteresis caused by water film at 10s.

3.2 Current-time curves of X65 carbon steel under different rotation speeds and alternate immersion periods

Figure 6 shows the typical current-time curves of the RCE electrode for alternate oil/water immersion under the static condition and various alternate immersion periods. As shown in Figure 6(a-c), the current-time curve obtained by 240 min potentiostatic polarisation can be explained by the frequency of current spikes. The spikes indicate that the measured current is larger than 0 mA, suggesting that the sample was in a water wetting state, otherwise, the measured current is 0 mA, which means that the sample surface was covered by an oil slug or film. Compared with the current-time curves under an alternate immersion period of 60 s, the frequency of current spikes was smaller under the immersion period of 5s and 10s, suggesting that the surface of the RCE electrode was easier to be covered by the oil film under a short alternate immersion period. The above observation is consistent with the magnified view (Part 5 of the *Appendix*) of the current-time curves at different time.

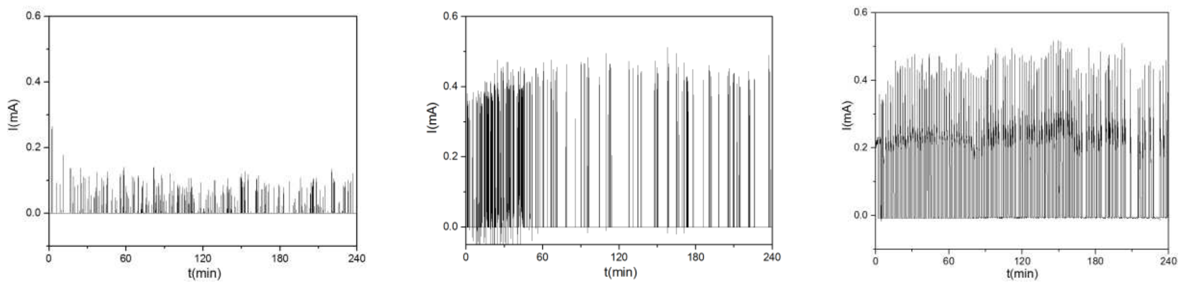

(a) (b) (c)

Figure 6. Typical current-time curves of the RCE electrode at the static condition in alternate oil/water slug with the alternate wetting periods of (a) 5s, (b) 10s, (c) 60s.

The current-time curves of the RCE sample at 500 rpm are shown in Figure 7. The characteristic of current-time curves at 500 rpm indicates a similar trend to that at the static state (Figure 6), suggesting that the low rotating speed has little influence on the wetting behaviour.

When the rotating speed was increased to 1000 rpm, the frequency of current spikes dramatically increased (Figure 8). It can be seen that no evident 0 mA current segments existed under the intermittent oil/water wetting with alternate immersion periods of 10 s and 60 s (Figure 8(b-c)). However, when the immersion period was dropped to 5s, 0 mA current areas appeared again (Figure 8(a)). The phenomenon implied that the rotating speed of 1000 rpm was high enough to change the wetting behaviour at the surface of the RCE electrode. However, a short alternate immersion period plays an important role in the wetting state of the sample during the alternate oil/water wetting process. With further increase of the rotating speed to 1500 rpm, there was no area of 0 mA current under the alternate wetting periods of not only 10s and 60s but also 5s (Figure 9). Even though the RCE electrode was immersed in an oil phase, the current was still above 0 mA. For more details of current-time curves, please see Part 5 of the *Appendix*, which shows the magnified view.

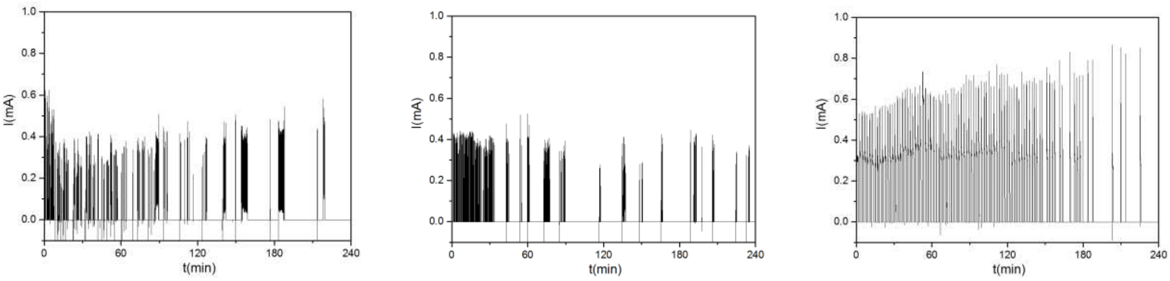

(a) (b) (c)

Figure 7. Typical current-time curves of the RCE electrode at 500rpm in alternate oil/water slug with the alternate wetting periods of (a) 5s, (b) 10s, (c) 60s.

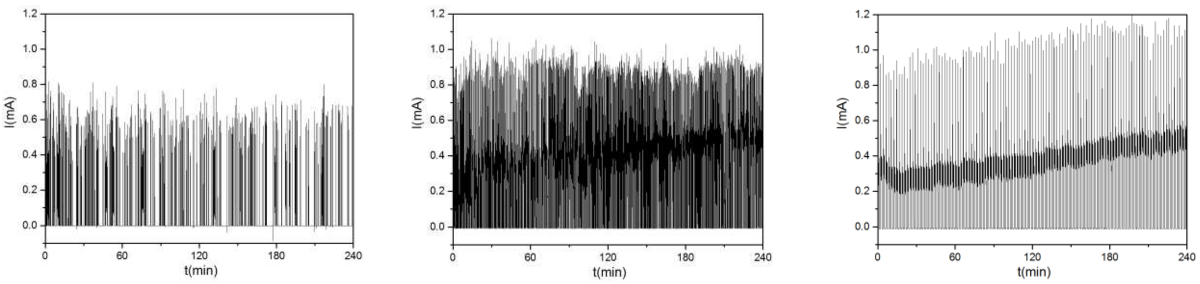

(a) (b) (c)

Figure 8. Typical current-time curves of the RCE electrode at 1000 rpm in the alternate oil/water slug with the immersion periods of (a) 5s, (b) 10s, (c) 60s.

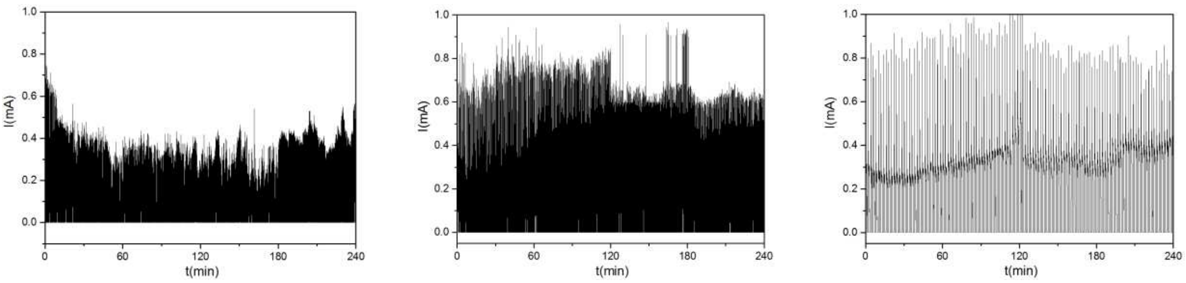

(a) (b) (c)

Figure 9. Typical current-time curves of the RCE electrode at 1500rpm in the alternate oil/water slug with the immersion periods of (a) 5s, (b) 10s, (c) 60s.

3.3. Corrosion morphology of X65 carbon steel under alternate oil/water wetting phenomena

Figure 10 indicates the SEM images of surface morphology on the surface of the RCE sample after 240 mins immersion in the CO_2-saturated solution (Figure 10(a)) and CO_2-saturated oil phase (Figure 10(b)) under the static conditions. The surface of the RCE electrode immersed in the CO_2-saturated solution was corroded after 240 mins (Figure 10(a)). However, as for the morphology of the electrode immersed in a CO_2-saturated oil phase, no corrosion was observed, and the grinding marks still appeared on the surface after 240 mins of exposure (Figure 10(b)).

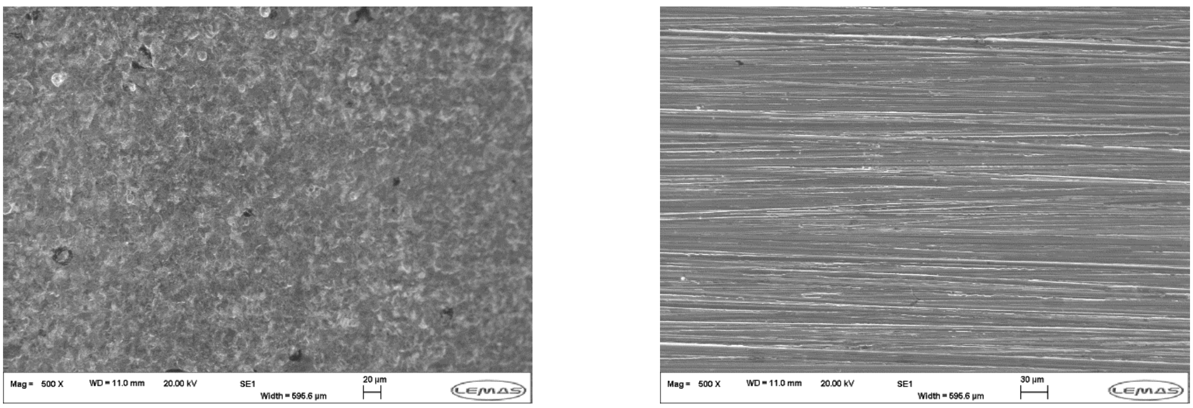

(a) (b)

Figure 10. Top-view SEM images of RCE electrode at 0rpm after 240 mins immersion test in the individual solution. (a) The CO_2-saturated aqueous solution, (b) CO_2-saturated oil.

Figure 11 shows the SEM images of surface morphology on the RCE sample surface under alternate oil and water immersions at various rotating speeds with the same alternate immersion period (10s). When the rotating speed was 500 rpm, the grinding marks were still visible on the surface (Figure 11(a)). The grinding marks became less apparent with the increase of rotating speed to 1000 rpm (Figure 11(b)). With further increase of rotating speed to 1500 rpm, polishing marks were disappeared, and the surface of the electrode suffered severe corrosion attack (Figure 11(c)). It is interesting to note that less corroded areas were observed randomly on the surface. Tying in with the earlier observation of fluidic behaviour of sample during intermittent wetting (Figure 5), this suggests that localised retained oil droplet can exist for a long time under turbulent condition.

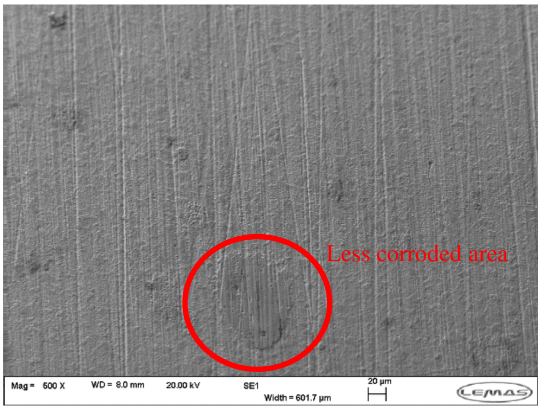

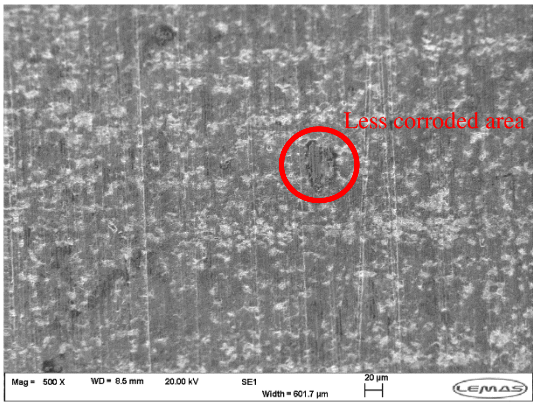

(a) (b)

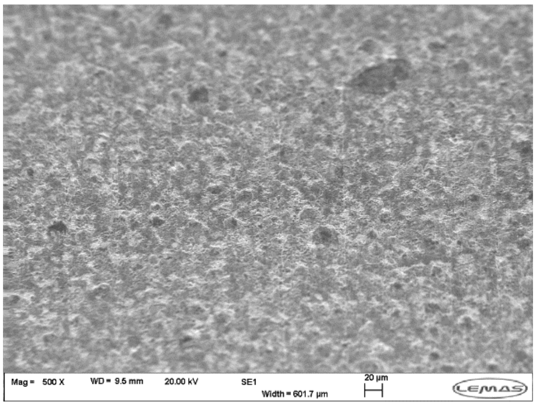

(c)

Figure 11. Top-view SEM images of RCE electrode at different rotating speed in the intermittent oil/water slug with the immersion periods of 10s (a) 500 rpm, (b) 1000 rpm, (c) 1500 rpm.

4. Discussion

4.1 A combined effect of flow velocity and alternate immersion period on the corrosion behaviour of carbon steel under alternate oil and water processes

Figure 12(a) shows a DME (Eq.1) comparison of the RCE electrode at different rotating speeds and alternate immersion periods. The higher DME represents more efficient corrosion mitigation. Under alternate oil/water wetting at the immersion period of 5s, the calculated DME at the static state was 98.7%, indicating that corrosion was significantly mitigated by the protective oil film on the surface. With the increase of rotating speed to 500, 1000 and 1500 rpm, DME sequentially reduced to 93.2%, 70.0% and 55.1% respectively, suggesting that the increase of flow velocity leads to more severe corrosion. When the alternate oil/water immersion period increased to 10s, DME at the static condition and 1500 rpm slightly dropped to 89.3% and 48.7% respectively and the DME at 1000 rpm dramatically reduced to 58%, suggesting that the lifetime of oil film on the surface becomes shorter as the increase in the flow speeds and resulting in a high corrosion rate. It should be noted that DME at 500, 1000 and 1500 rpm is consistent with corrosion morphology (Figure 11).

Besides, with the further increase of the alternate oil/water wetting period to 60s, DME at the static condition and 500 rpm dropped to 60%, and DME at 1000 and 1500rpm remained at 50%. The results indicate that the corrosion behaviour of carbon steel under alternate oil/water wetting processes is determined by the combined effect of rotating speeds and alternate oil/water immersion periods. A low rotating speed, resulting in the efficiently mitigated corrosion under a short alternate oil/water wetting period, such as 5s. However, when the rotating speed is high (1500 rpm), the corrosion mitigation efficiency under different immersion periods is similar.

Figure 12(b) illustrates the ratio between oil wetting time and water wetting time (θ, Eq.2) under different rotating speeds and immersion periods, which reflects the wetting state of the electrode under the intermittent oil/water wetting. When the alternate oil/water immersion period was 5s, θ of 23.48 was calculated at the static condition, which was larger than that of θ at other rotating speeds. The values of θ at 500 and 1000 rpm were bigger than 1, indicating that the oil wetting time was larger than the water wetting time. On the contrary, θ at 1500 rpm was 0.98, suggesting that the high corrosion rate is attributed to the long water wetting time.

With the increase of the alternate oil/water immersion period to 10s, θ at 500 rpm increased to 21.43, however, θ at the static condition and 1000 rpm decreased to 5.9 and 1.3 respectively. When the alternate oil/water immersion period further increased to 60s, θ at different rotating speeds were close to 1. Figure 12(c) shows a correlation between DME and θ obtained in the present research, which was established by using logistic regression analysis [36]. The calculated R-square number was 0.908, suggesting a strong correlation between corrosion behaviour and the wetting state of the electrode in intermittent wetting. When θ was located in the region from 0 to 8, the DME significantly increased to about 100% with the rise of θ. When θ was above 8, the DME slightly approached 100%.

According to the histogram of the oil or water film lifetime (Part 6 in *Appendix*), the increase in the rotating speed or extension of the alternate oil/water immersion period, resulted in the decrease of the lifetime of the oil film formed on the surface, which consequently reduces the DME and θ. Therefore, the corrosion behaviour under the long-term intermittent oil/water wetting phenomenon is determined by the lifetime of oil/water film after each transition of the immersion state.

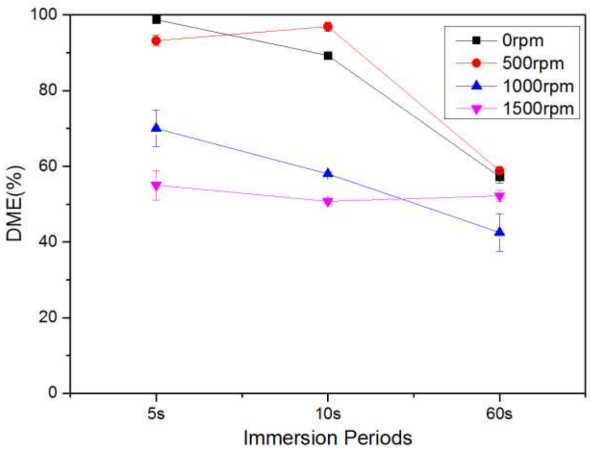

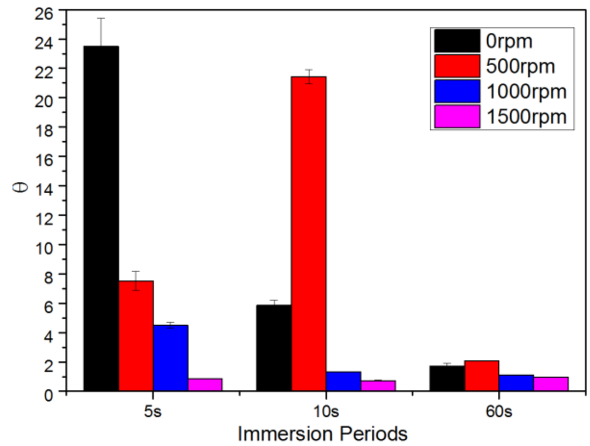

(a) (b)

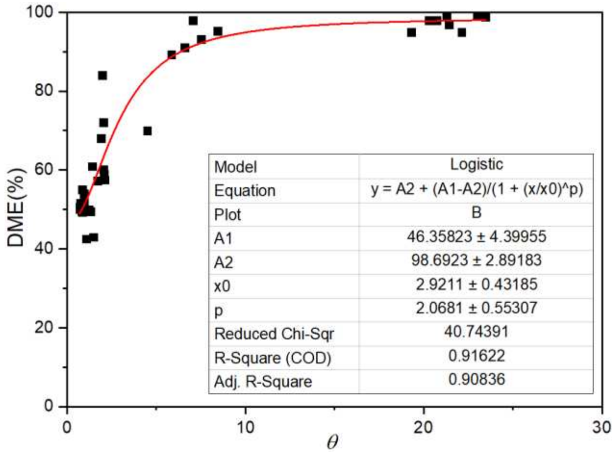

(c)

Figure 12. Statistical data of RCE electrode under alternate oil/water wetting with different flow conditions. (a) DME as a function of the alternate oil/water wetting period and rotating speed, (b) ratio between oil wetting time and water wetting time (θ) as a function of alternate oil/water wetting period and rotating speed, (c) correlation between DME and θ obtained at all flow condition.

4.2 Wetting hysteresis under alternate oil/water wetting processes

Figure 13 shows the oil/water interface around a static RCE electrode under intermittent wetting. Firstly, the concave meniscus of the oil/water interface under the equilibrium state indicates that carbon steel was hydrophilic at the static state (Figure 13(a)). With the rise of the oil/water interface, the meniscus shape has changed to convex with the increase of contact angle (Figure 13(b)), which leads to the entrainment of oil in the water slug (Figure 13(d), Video7 in Part4 of the *Appendix*). On the contrary, when the oil/water interface dropped, the meniscus shape became convex and more water was trapped in the meniscus (Figure 13(c)). According to previous research [35, 37-41], the observed thin film is called Landau-Levich film, which is formed under a large contact line velocity. The contact line velocity in the present experiment is 8 mm/s, which is smaller than near-wall flow velocity in an oilfield pipeline [42-43]. Therefore, it is reasonable to propose that the thin-film exists in the inner surface of the pipe.

Champougny's research [35] found that the lifetime of thin-film is proportional to the critical thickness of the film, and the thickness of oil/water film increases with Capillary number ($Ca = \frac{\eta V}{\gamma}$) [41]. In the present paper, contact line velocity V and surface tension between oil and water γ are constant, the viscosity of water or oil is different. Therefore, the large viscosity of oil leads to a longer lifetime of oil film on the surface as well as the oil wetting time under intermittent oil/water wetting. Besides, when the rotating speed increases, high shear stress lead to a thinner oil film thickness and results in the reduction of the lifetime of the protective oil film formed on the surface.

Besides, when the sample was pre-wetted by the oil film, the meniscus of the oil/water interface became convex at the equilibrium state (Figure 13(e)). The pre-wetted oil film caused the receding contact angle larger than that of without pre-wetted oil film (Figure 13(f), Video7 of the *Appendix*), suggesting a pre-wetted oil film renders the surface more oleophilic and promotes long lifetime of the oil film during alternate wetting.

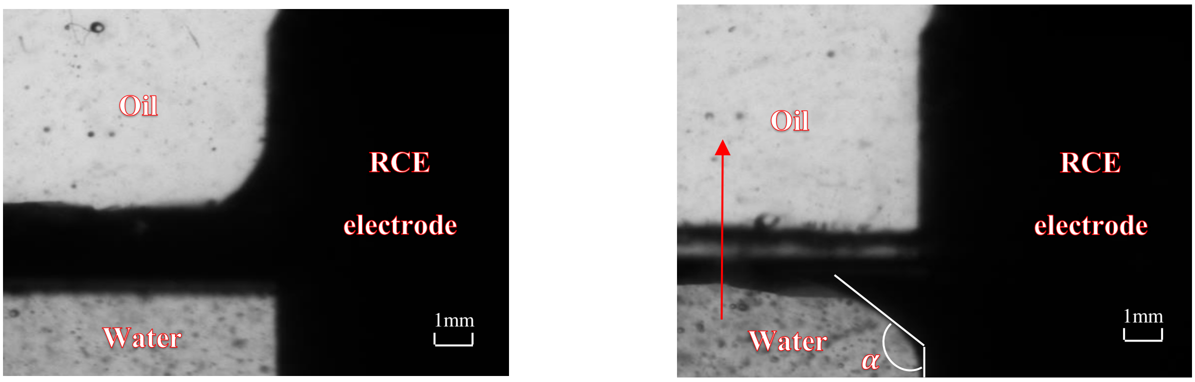

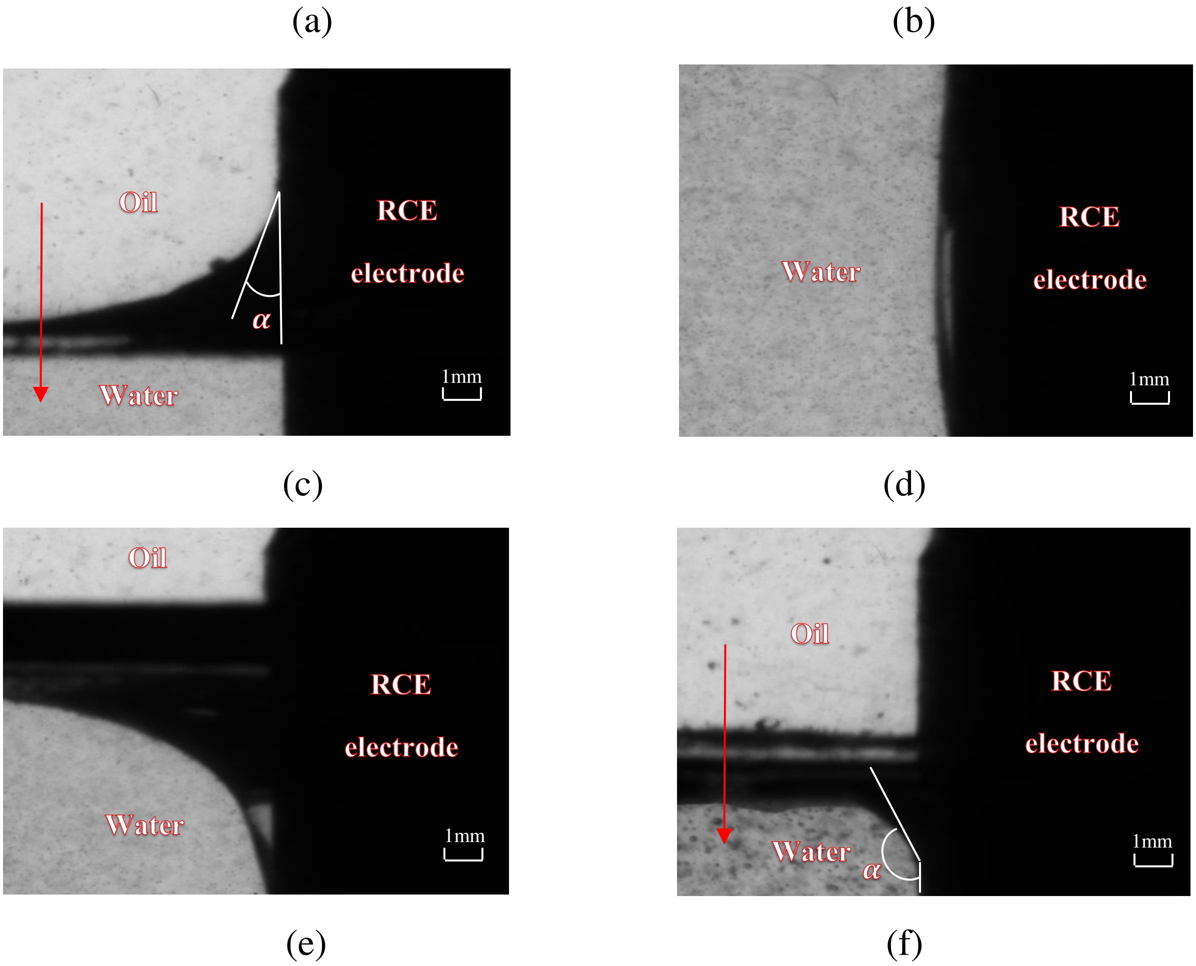

Figure 13. Observation of meniscus shape near a static RCE electrode at different flow state. (a) equilibrium state, (b) rise of oil/water interface, (c) drop of oil/water interface, (d) after transitioning from oil immersion to water immersion, (e) equilibrium state when electrode pre-wetted by an oil film, (f) drop of oil/water interface when electrode pre-wetted by an oil film.

4.3 Corrosion characterisation of carbon steel under intermittent oil/water wetting

The statistical analysis as shown in Figure 12 indicates that the current-time curves under various rotating speeds and immersion periods reflect the corrosion behaviour of carbon steel. The corrosion mitigation efficiency indicates a proportional correlation to the ratio between oil wetting time and water wetting time. The observation of corrosion morphology (Figure 10) confirms that the corrosion reactions are mainly contributed from the water film covered on the surface during the intermittent wetting processes.

However, water wetting time on the surface is strongly affected by the wetting hysteresis under intermittent oil/water wetting. According to the observation of fluidic behaviour, wetting hysteresis is attributed to the formation of thin oil/water film on the surface during the transition between oil immersion and water immersion. The present research shows that the alternate oil/water immersion periods and flow velocities affect the lifetime of the water/oil films on the surface. Besides, statistical data of the current-time curve of carbon steel under alternate oil/water wetting processes with different immersion periods (Figure S7 in Part 6 of the *Appendix*) shows that a short immersion period can change the lifetime of the films on the surface. For example, the peak lifetime of the oil film formed on the surface of the electrode under the static condition at an alternate oil/water immersion period of 60s was in the ranges of 0-1s, compared with that of the oil film for 5s at the period of 5s (Figure S7(a) in Part 6 of the *Appendix*).

A short alternate oil/water immersion period increases the lifetime of the oil film due to the formation of the oil film is easier to coalesce with the bulk oil, stabilising the oil film on the surface. The above hypothesis can be ascertained by the current-time curves. When the alternate oil/water immersion periods are 10s and 60s, the peak lifetime of the oil film on the surface was calculated in the ranges of 3-4s. With the reduction of the alternate oil/water wetting period to 5s, the peak lifetime increased to 4-5s. However, when the rotating speed is too high, the alternate oil/water immersion period doesn't affect the lifetime of the thin-film formed on the surface.

5. Conclusion

The corrosion behaviour of carbon steel under intermittent oil/water wetting at different rotating speeds and alternate oil/water immersion periods were systematically investigated by a new and simple "alternate wetting cell".

1. Wetting hysteresis under intermittent wetting is caused by the formation of thin oil/water film on the surface during the transition between oil immersion and water immersion.
2. When the ratio (θ) between oil wetting time and water wetting time was smaller than 8, the DME significantly increased to about 100% with the rise of θ. When θ was above 8, the DME slightly approached 100%.
3. The corrosion behaviour of carbon steel under intermittent wetting was controlled by the lifetime of oil film, which is formed by the dynamic movement of the contact line on the steel surface. The lifetime is dependent on the combined effect of the rotating speeds and alternate oil/water immersion periods.
4. Compared with a low rotating speed (0 or 500 rpm), higher shear stress at 1000 and 1500 rpm leads to a shorter lifetime of oil film on the surface, which therefore decreases corrosion mitigation efficiency.

5. The observation of corrosion morphology suggests that small un-corroded islands can exist, highlighting a local tenacity of oil film even under turbulent intermittent oil/water wetting.

Data Availability

The processed data required to reproduce these findings cannot be shared at this time as the data also forms part of an ongoing study.

CRediT authorship contribution statement:

Wenlong Ma: Conceptualization, Methodology, Software, Formal analysis, Investigation, Data Curation, Writing – Original Draft, Visualization

Hanxiang Wang: Conceptualization, Writing – Review & Editing, Supervision

Nikil Kapur: Resources, Writing – Review & Editing, Interpretation, Supervision

Richard Barker: Resources, Writing – Review & Editing, Interpretation, Supervision

Yong Hua: Methodology, Resources, Writing – Review & Editing, Supervision

Anne Neville: Conceptualization, Methodology, Resources, Supervision, Funding acquisition

Acknowledgements:

The first author is sponsored by the Graduate School in China University of Petroleum (East China) and the Institute of Functional Surface in University of Leeds.

Reference:

1. Al-Janabi, Yahya T. "An Overview of Corrosion in Oil and Gas Industry: Upstream, Midstream, and Downstream Sectors." Corrosion Inhibitors in the Oil and Gas Industry (2020): 1-39.

2. Ilman, M. N. "Analysis of internal corrosion in subsea oil pipeline." case studies in Engineering Failure Analysis 2, no. 1 (2014): 1-8.

3. Papavinasam, S., A. Doiron, T. Panneerselvam, and R. W. Revie. "Effect of hydrocarbons on the internal corrosion of oil and gas pipelines." Corrosion 63, no. 7 (2007): 704-712.

4. Choi, H. J., R. L. Cepulis, and J. B. Lee. "Carbon dioxide corrosion of L-80 grade tubular in flowing oil-brine two-phase environments." Corrosion 45, no. 11 (1989): 943-950.

5. Rashedi, Ahmadreza. "A Study of Surface Wetting in Oil-Water Flow in Inclined Pipeline." PhD diss., Ohio University, 2016.

6. Lotz, U., L. Van Bodegom, and C. Ouwehand. "The effect of type of oil or gas condensate on carbonic acid corrosion." Corrosion 47, no. 8 (1991): 635-645.

7. Al-Hashem, AbdulHameed, and John A. Carew. "CO_2 corrosion of L-80 steel in simulated oil well conditions." In CORROSION 2002. OnePetro, 2002.

8. Cui, Z. D., S. L. Wu, C. F. Li, S. L. Zhu, and X. J. Yang. "Corrosion behavior of oil tube steels under conditions of multiphase flow saturated with super-critical carbon dioxide." Materials letters 58, no. 6 (2004): 1035-1040.

9. Farelas, Fernando, Yoon-Seok Choi, S. Nešić, Alvaro Augusto O. Magalhães, and Cynthia de Azevedo Andrade. "Corrosion Behavior of Deep Water Oil Production Tubing Material Under Supercritical CO_2 Environment: Part 2—Effect of Crude Oil and Flow." Corrosion 70, no. 2 (2013): 137-145.

10. Sun, Jianbo, Chong Sun, Guoan Zhang, Weimin Zhao, and Yong Wang. "Effect of water cut on the localized corrosion behavior of P110 tube steel in supercritical CO_2/oil/water environment." Corrosion 72, no. 11 (2016): 1470-1482.

11. Wang, Zi Ming, An Qing Liu, Xia Han, Xing Zhang, Lin Zhao, Jian Zhang, and Guang-Ling Song. "Fluid structure governing the corrosion behavior of mild steel in oil–water mixtures." Corrosion Engineering, Science and Technology 55, no. 3 (2020): 241-252.

12. Becerra, Haydée Quiroga, C. Retamoso, and Digby D. Macdonald. "The corrosion of carbon steel in oil-in-water emulsions under controlled hydrodynamic conditions." Corrosion Science 42, no. 3 (2000): 561-575.

13. Efird, K. D., and R. J. Jasinski. "Effect of the crude oil on corrosion of steel in crude oil/brine production." Corrosion 45, no. 2 (1989): 165-171.

14. Castillo, Marta, Jose R. Vera, Hernan Rincon, Simona Duplat, and Evaristo Baron. "Protective properties of crude oils in CO_2 and H_2S corrosion." In CORROSION 2000. OnePetro, 2000.

15. Biomorgi, J., S. Hernández, J. Marín, E. Rodriguez, M. Lara, and A. Viloria. "Internal corrosion studies in hydrocarbons production pipelines located at Venezuelan Northeastern." Chemical Engineering Research and Design 90, no. 9 (2012): 1159-1167.

16. Craig, Bruce. "Predicting the conductivity of water-in-oil solutions as a means to estimate corrosiveness." Corrosion 54, no. 8 (1998): 657-662.

17. Cai, J. Y., Srdjan Nesic, Chong Li, Xuanping Tang, Francois Ayello, Ivan Cruz, and Jamal Khamis. "Experimental studies of water wetting in large diameter horizontal oil-water pipe flows." In SPE Annual Technical Conference and Exhibition. OnePetro, 2005.

18. Li, Chong, Xuanping Tang, Francois Ayello, Jiyong Cai, Srdjan Nesic, C. Ivan T. Cruz, and Jamal N. Al-Khamis. "Experimental study on water wetting and CO_2 corrosion in oil-water two-phase flow." NACE Corrosion 6595 (2006).

19. Tang, Xuanping. "Effect of surface state on water wetting and carbon dioxide corrosion in oil-water two-phase flow." PhD diss., Ohio University, 2011.

20. Kee, Kok Eng. "A study of flow patterns and surface wetting in gas-oil-water flow." PhD diss., Ohio University, 2014.

21. Schmitt, Guenter, Gilda Karbasi, Srdjan Nešic, Rudolf Hausler, Brian Kinsella, and Bruce Brown. "Pitting in the water/hydrocarbon boundary region of pipelines-Effect of corrosion inhibitors." In NACE-International Corrosion Conference Series. 2013.

22. Liu, Enbin, Bingyan Guo, Mingjun Wang, Xi Ma, and Yong Peng. "Analysis of the water‐filling process for crude oil pipelines with a large drop in height." Energy Science & Engineering 8, no. 6 (2020): 2100-2115.

23. Nešić, S., and F. Carroll. "Horizontal rotating cylinder—a compact apparatus for studying the effect of water wetting on carbon dioxide corrosion of mild steel." Corrosion 59, no. 12 (2003): 1085-1095.

24. Babic, Marijan. "Role of Interfacial Chemistry on Wettability and Carbon Dioxide Corrosion of Mild Steels." PhD diss., Ohio University, 2017.

25. Wang, Zi Ming, Qing Yu Lun, Jian Wang, Xia Han, Wei Zhu, Jian Zhang, and Guang-Ling Song. "Corrosion mitigation behavior of an alternately wetted steel electrode in oil/water media." Corrosion Science 152 (2019): 140-152.

26. Luo, Xiaoming, Guobin Lü, Wei Zhang, Limin He, and Yuling Lü. "Flow structure and pressure gradient of extra heavy crude oil-water two-phase flow." Experimental Thermal and Fluid Science 82 (2017): 174-181.

27. Liu, G., D. A. Tree, and M. S. High. "Relationships between rotating disk corrosion measurements and corrosion in pipe flow." Corrosion 50, no. 8 (1994): 584-593.

28. Bonn, Daniel, Jens Eggers, Joseph Indekeu, Jacques Meunier, and Etienne Rolley. "Wetting and spreading." Reviews of modern physics 81, no. 2 (2009): 739.

29. de Castro, T. C. "Forensic Interpretation of Bloodstains on Fabrics." In Forensic Textile Science, pp. 127-167. Woodhead Publishing, 2017.

30. Härting, Hans-Ulrich, André Bieberle, Rüdiger Lange, Faïçal Larachi, and Markus Schubert. "Hydrodynamics of co-current two-phase flow in an inclined rotating tubular fixed bed reactor—Wetting intermittency via periodic catalyst immersion." Chemical Engineering Science 128 (2015): 147-158.

31. Zong, Yan-Bo, Ning-De Jin, Zhen-Ya Wang, Zhong-Ke Gao, and Chun Wang. "Nonlinear dynamic analysis of large diameter inclined oil–water two phase flow pattern." International Journal of Multiphase Flow 36, no. 3 (2010): 166-183.

32. Nešic, S., G. Th Solvi, and J. Enerhaug. "Comparison of the rotating cylinder and pipe flow tests for flow-sensitive carbon dioxide corrosion." Corrosion 51, no. 10 (1995): 773-787.

33. Walfish, Steven. "A review of statistical outlier methods." Pharmaceutical technology 30, no. 11 (2006): 82.

34. Ortega-Toledo, D. M., J. G. Gonzalez-Rodriguez, M. Casales, L. Martinez, and A. Martinez-Villafañe. "CO_2 corrosion inhibition of X-120 pipeline steel by a modified imidazoline under flow conditions." Corrosion Science 53, no. 11 (2011): 3780-3787.

35. Champougny, Lorène, Emmanuelle Rio, Frédéric Restagno, and Benoit Scheid. "The break-up of free films pulled out of a pure liquid bath." Journal of fluid mechanics 811 (2017): 499-524.

36. Pearson, Karl. "VII. Note on regression and inheritance in the case of two parents." proceedings of the royal society of London 58, no. 347-352 (1895): 240-242.

37. Al-Shareef, Amer, Partho Neogi, and Baojun Bai. "Force based dynamic contact angles and wetting kinetics on a Wilhelmy plate." Chemical Engineering Science 99 (2013): 113-117.

38. Quéré, David. "Fluid coating on a fiber." Annual Review of Fluid Mechanics 31, no. 1 (1999): 347-384.

39. Maleki, M., M. Reyssat, F. Restagno, D. Quéré, and Christophe Clanet. "Landau–levich menisci." Journal of colloid and interface science 354, no. 1 (2011): 359-363.

40. Snoeijer, Jacco H., and Bruno Andreotti. "Moving contact lines: scales, regimes, and dynamical transitions." Annual review of fluid mechanics 45 (2013).

41. Rio, Emmanuelle, and François Boulogne. "Withdrawing a solid from a bath: How much liquid is coated?." Advances in colloid and interface science 247 (2017): 100-114.

42. Nešić, Srdjan. "Key issues related to modelling of internal corrosion of oil and gas pipelines–A review." Corrosion science 49, no. 12 (2007): 4308-4338.

43. Kumara, W. A. S., G. Elseth, B. M. Halvorsen, and M. C. Melaaen. "Comparison of Particle Image Velocimetry and Laser Doppler Anemometry measurement methods applied to the oil–water flow in horizontal pipe." Flow measurement and Instrumentation 21, no. 2 (2010): 105-117.